Variational Monte Carlo study of the partially polarized electron gas

Warren E. Pickett and Jeremy Q. Broughton
Complex Systems Theory Branch, Code 6690, Naval Research Laboratory, Washington, D.C. 20375-5345
(Received 22 March 1993; revised manuscript received 16 August 1993)

The variational Monte Carlo (VMC) method, using Jastrow-Slater (JS) wave functions, is used to study the partially polarized interacting electron gas for densities spanning the range encountered in bulk metals. We concentrate on a spin polarization $\zeta=0.42$ which allows direct comparison of polarized and unpolarized states for a fixed total number of electrons in the simulation supercell. The radial distribution functions $g_{++}(r)$, $g_{--}(r)$, and $g_{+-}(r)$ are given particular attention and compared with a model developed by Perdew and Wang (PW) that satisfies known constraints. At high density the agreement with the PW model is good. At the lower densities (electron-gas parameter $r_s=4$–8) there are differences that can be roughly characterized as the PW model giving a somewhat more extended exchange-correlation hole than the VMC calculations. These discrepancies could be due to limitations either of the PW model or of the JS wave functions used here. Both the VMC and PW results are contrasted with the Hartree-Fock result for parallel spins.

I. INTRODUCTION

The variational Monte Carlo (VMC) method[1] is a straightforward and appealing approach for investigating quantum systems. One posits a many-body wave function, typically involving several parameters to be determined by minimizing the resulting energy, and then one can calculate (at least in principle) a wide variety of characteristics of the state described by the wave function. The VMC method has been applied to a number of atoms and molecules,[2] and to condensed matter systems,[3] as well as being implemented in the study of model Hamiltonians for such systems.

For extended condensed matter systems, the simplest and yet most fundamental model is the interacting homogeneous electron gas (HEG). The understanding of the HEG is crucial, not least because it forms the basis of the widely used and highly successful local density approximation to the exchange-correlation potential that arises in density-functional theory (DFT). Both the unpolarized HEG and the completely spin-polarized HEG have been studied not only by the VMC method[1] but also by Green's-function-based quantum Monte Carlo methods[4,5] that are more accurate. As a result of these studies the dependence on the density $n(r)$ of the correlation energy $E_c[n]$ of these two limiting cases of the HEG is known. Only scarce reports of the radial distribution function (RDF), or equivalently the exchange-correlation hole reflecting the correlation of pairs of electrons, are available,[6] and again only for the unpolarized or fully polarized cases.

For intermediate polarizations $0<\zeta<1$ [with the definition $\zeta=(n_+-n_-)/(n_++n_-)$ in terms of the majority and minority electron densities, n_+ and n_-, respectively] little has been learned explicitly about the correlation energy $E_c[n,\zeta]$ except some limiting behaviors, and even less is known about the RDF. Recently Perdew and Wang[7] have combined the available knowledge concerning the partially polarized HEG with some formal expressions to construct approximate analytic expressions for the RDF's $g_{ss'}(r)$, $s,s'=+$ or $-$, which give the probability of finding an electron of spin s' at distance r given that there is an electron of spin s at the origin. Since $E_c[n,\zeta]$ can be written (see, for example, Ref. 7) in terms of a coupling constant average of $g_{ss'}$ (where the coupling constant refers to the "turning on" of interactions between electrons) the correlation energy and the RDF are intimately related. Very recently Ortiz and Ballone[8] have reported VMC and fixed-node diffusion quantum Monte Carlo studies of the partially polarized electron gas. Their results for correlation energies are consistent with the more refined interpolations that are currently in use.

Contrary to the modest amount of effort expended in evaluating the RDF is its fundamental status in the density-functional theory of inhomogeneous electronic systems. The (unknown) exchange-correlation energy functional $E_{xc}[n]$ is directly formulated in terms of the (coupling constant average of the) exchange-correlation hole. The considerable success of the local density approximation (LDA) to DFT is understood in terms of two important features of the spherical exchange-correlation hole that arises in LDA: (1) it is properly normalized to account for a single unit charge, and (2) the energy depends only on the spherical average anyway, so that anisotropic behavior is not so important. Here we consider a question that has received virtually no attention to date: what is the dependence on polarization of the RDF's in the electron gas? Future more reliable implementations of DFT are likely to require these RDF's as input.

In this study we make the initial step in applying the VMC method to address these questions. We have chosen the VMC method, rather than some other quantum Monte Carlo method, in anticipation of investigating better wave functions in the future (incorporating, for example, three-body correlations). In principle, deficiencies in the calculated RDF's could be used directly to suggest corrections to the Jastrow factor; in practice, all we have

to compare with is the Perdew-Wang model, and it is not clear yet how accurate it is, especially for intermediate polarizations.

In Sec. II we discuss some features of the VMC method related to our implementation. As we will discuss in Sec. III, it is not at all a simple matter to investigate arbitrary spin polarizations at a given density, which accounts for the lack of such studies in the past. Results are presented in Secs. IV and V, and a discussion and comparison with known results is provided in Sec. VI.

II. METHOD OF CALCULATION

The point of departure of the VMC method is the many-body wave function, which as usual we take to be of the (unnormalized) Jastrow-Slater form

$$\Psi(\{r_{i,+}\},\{r_{j,-}\})=J(\{r_{i,+}\},\{r_{j,-}\}) \times D_+(\{r_{i,+}\})D_-(\{r_{j,-}\}) , \quad (1)$$

where D_+ and D_- are the majority and minority Slater determinants of the free-electron gas that enforce an antisymmetric wave function. The Jastrow factor is a symmetric coefficient that can be written as

$$J=J_{++}J_{--}J_{+-}J_{-+} \quad (2)$$

in terms of the partial Jastrow factors

$$J_{ss'}=\exp\left[-\tfrac{1}{2}\sum_{i=1}^{N_s}\sum_{i'=1}^{N_{s'}}u_{ss'}(|r_{is}-r_{i's'}|)\right] =\exp[-U_{ss'}] . \quad (3)$$

Here N_s is the number of particles of spin s ($=+$ or $-$). Note that $J_{+-}=J_{-+}$.

The Coulomb nature of the electron gas dictates that $u_{ss'}(r)\sim 1/r$ at large distances. This form has the immediate consequence that one cannot cut off the summations at a finite distance, a fact that had led practitioners to apply supercell techniques to model the HEG. We follow this practice. Since $u_{ss'}$ can be written as

$$u_{ss'}(r)=\frac{A}{r}+w_{ss'}(r) , \quad (4)$$

where A is a constant and $w_{ss'}$ is short ranged, the standard practice is to handle the A/r factor as the e^2/r Coulomb repulsion is handled (although it is conceptually quite distinct), by subtracting out a term that mathematically looks like a compensating factor of opposite sign. The result is an Ewald expression just like the one that occurs in handling the Coulomb interaction,[1,3,9] plus the $w_{ss'}$ term which is short ranged and therefore can be treated in real space.

In the VMC method one wishes to sample with a random walk the local energy

$$\frac{H\Psi(R)}{\Psi(R)}=T_{\rm loc}+V(R) =\left[-\frac{\hbar^2}{2m}\sum_i\nabla_i^2\Psi(R)\right]\Big/\Psi(R)+V(R) , \quad (5)$$

where R denotes the set of electron coordinates. The Markovian walk through electronic configuration space was generated using the standard Monte Carlo sampling algorithm of Metropolis *et al.*[10] Determinant evaluations and updates were performed using an N^2 algorithm rather than the brute force N^3; similar techniques are described in Refs. 1 and 3. This speed advantage is possible because each attempted primitive move changes merely a single row in the determinant.

The interelectronic repulsion Coulomb term $V(R)$ and compensating positive background are evaluated with standard Ewald methods and will not be discussed further here. The local kinetic energy is given by

$$T_{\rm loc}=T_0+\sum_{is}t_{c,is} , \quad (6)$$

where T_0 is the determinantal (free-electron) kinetic energy, and the correlation contribution to the local kinetic energy t_c of the $\{is\}$ electron is

$$t_{c,is}=\frac{\hbar^2}{2m}[\nabla_{is}^2U-|\nabla_{is}U|^2+2\nabla_{is}U\cdot\nabla_{is}D_s] . \quad (7)$$

We have used the form of "pseudopotential"

$$u_{ss'}(r)=\frac{A}{r}(1-e^{r/b_{ss'}}) , \quad (8)$$

where $A=e^2/\hbar\omega_p=(r_s^3/3a_B)^{1/2}$ independent of relative spin satisfies the plasmon constraint, and $b_{++}=b_{--}=(2A)^{1/2}$, $b_{+-}=b_{-+}=A^{1/2}$ satisfy the cusp condition for parallel and antiparallel spin electrons, respectively. There is no fundamental reason why an approximate variational wave function should be required to satisfy these conditions precisely, but allowing their variation has been found not to result in any noticeable lowering of the energy. Form (8) has been used by Ceperley[1] for the electron gas (with a spin-independent value of $b_{\sigma\sigma'}$) and by Louie and co-workers[3,11–13] to study diamond, silicon, and solid hydrogen.

For this form of pseudopotential the first term of Eq. (7) is everywhere negative, and the second term is explicitly negative. The third term, and the net value, may be of either sign. Ceperley[1] has noted that the kinetic energy can be written, and evaluated, in various ways. Defining the quantities

$$T=-\frac{\hbar^2}{2m}\tfrac{1}{2}\nabla^2\ln\Psi , \quad (9)$$

$$F=\frac{\hbar}{\sqrt{2m}}\nabla\ln\Psi , \quad (10)$$

$$K\equiv T_{\rm loc}=2T-F^2 , \quad (11)$$

one can show that

$$\langle K\rangle=\langle T\rangle=\langle F^2\rangle . \quad (12)$$

While these must all have the same mean value over the random walk regardless of the wave function, they can have quite different variances depending on the quality of the wave function. Since one interest is to explore the quality of this variational wave function, we have monitored the mean values and variances for the different ex-

pressions. We have verified that K has much the smallest variance of the three possibilities K, T, and F^2 (see Sec. VI).

III. SUPERCELLS AND NUMBER OF ELECTRONS IN THE SIMULATIONS

We have used simple cubic supercells repeated in three dimensions, which allows one to include effects of the long-range Coulomb interaction at the cost of constraining the system by the resulting artificial periodicity. Tests using progressively larger supercells and finite-size scaling of the resulting quantities (principally energies) are required to assess and try to eliminate supercell effects. The alternative is to treat a finite volume. However, in a typical simulation with $5\times5\times5=125$ electrons, all but $\sim3\times3\times3=27$ would be surface electrons not sampling a bulk environment, which clearly is unacceptable. Thus obtaining bulk properties from a finite volume is not feasible without periodic boundary conditions.

The plane-wave states $\phi(r)=\exp(i\mathbf{G}\cdot\mathbf{r})$ that go into the Slater determinants are labeled with supercell reciprocal-lattice vector $\mathbf{G}$. Rotational and translational symmetry requires that complete shells ("stars") of G states be occupied if any member is occupied, and expectations (and experience) dictate that the plane-wave states with small kinetic energies G^2 be occupied first. To avoid complex determinants we use sines and cosines rather than plane waves. In our simple cubic lattice of supercells the allowed numbers of electrons of either spin are 1, 7, 19, 27, 33, 57, 81, 93, 99, 123, 147, 171, 179, ... Thus one is allowed only discrete numbers of majority and minority electrons per supercell, and therefore discrete values of the polarization ζ, although the density can be varied arbitrarily by adjusting the lattice constant.

This discreteness has inhibited studies of the partially polarized HEG, since it is impossible to carry out calculations of different polarizations at a given density for fixed number of particles N in the supercell, or to do finite-size scaling at a fixed polarization. An exception to the first difficulty is the "magic" combination $57+57=114=81+33$. This allows a *direct* comparison of simulations with 114 total electrons, first unpolarized and then with polarization $(81-33)/114=0.421$. We will concentrate primarily on this "magic" case. Supercell (finite-size) effects cannot be eliminated, but are minimized because the number of electrons is identical. We discuss supercell effects on the RDF's below.

IV. RADIAL DISTRIBUTION FUNCTION

The RDF $g_{ss'}(r)$ is defined as the probability that there is an electron of spin s' at a distance r from a given electron of spin s taken to be at the origin. It is normalized so that it becomes unity at large distances. The RDF is important because it is a direct manifestation of the correlation between pairs of electrons, and plays a fundamental role in the theory of the correlation energy.

Several features of the RDF are known. The parallel-spin RDF represents an exchange-correlation hole containing one unit of charge, while the antiparallel spin RDF reflects only a redistribution of electrons:

$$\int[1-g_{ss'}(r)]4\pi r^2dr=\delta_{ss'}\ . \tag{13}$$

The total RDF (averaged over relative spins) is given by

$$g(r)=\left[\frac{1+\zeta}{2}\right]^2 g_{++}(r)+\left[\frac{1-\zeta}{2}\right]^2 g_{--}(r) +2\frac{1+\zeta}{2}\frac{1-\zeta}{2}g_{+-}(r)\ . \tag{14}$$

The Kato-Kimball[14,15] cusp condition is

$$\frac{dg}{dr}(r=0)\equiv g'(0)=\frac{1}{a_0}g(0)\ , \tag{15}$$

and since antisymmetry of the wave function with respect to electron coordinates requires both $g_{ss}(0)$ and $g'_{ss}(0)$ to vanish, this translates into a condition on g_{+-} alone. Here $a_0=\hbar^2/me^2$ is the usual Bohr radius.

Rajagopal, Kimball, and Banerjee[16] (RKB) have derived a further condition on the parallel spin RDF:

$$g''_{ss}(0)=\tfrac{2}{3}a_0 g'''_{ss}(0)\ . \tag{16}$$

Combined with $g_{ss}(0)=0=g'_{ss}(0)$, this constrains the small-r behavior to be

$$g_{ss}(r)=\tfrac{1}{2}g''_{ss}(0)\left[r^2+\frac{1}{2a_0}r^3+\cdots\right], \tag{17}$$

$$g_{+-}(r)=g_{+-}(0)\left[1+\frac{r}{a_0}+\cdots\right], \tag{18}$$

where $g''_{ss}(0)$ and $g_{+-}(0)$ must be determined by calculation. RKB have emphasized that in the paramagnetic and partially polarized electron gases the energy is particularly sensitive to the antiparallel RDF, and is less sensitive to the parallel spin RDF's because they are strongly constrained by Fermi statistics to be small where the Coulomb repulsion is largest. The present calculations allow the determination of the constants in Eqs. (17) and (18), and these values and analysis of the small-distance behavior will be provided in a separate paper.

The RDF's displayed in this paper were calculated by sampling the configurations during the VMC runs; typically sampling was done each $\sim N/2$ attempted steps, where N is the number of particles in the supercell. The RDF's were collected on a histogram of width $\Delta x=\Delta(r/r_s)=0.02$ in the range $0<x\leq4$ over a total of 5×10^5 total attempts. For a maximum step size chosen to be $1.15r_sa_0$ the acceptance ratio was $\sim60\%$. An example of the "raw data" thus generated is shown in Fig. 1 for $r_s=8$. [r_s is the conventional electron-gas parameter: in terms of the density n, $(4\pi/3)(r_sa_0)^3=1/n$.] Note that for the spin-polarized case the parallel minority-spin RDF $g_{--}(r)$ is noticeably more noisy than $g_{+-}(r)$ and (especially) $g_{++}(r)$ (there are $81^2/33^2\approx6$ more $++$ pairs as $--$ pairs). The RDF's were smoothed for presentation in subsequent figures with an approximately

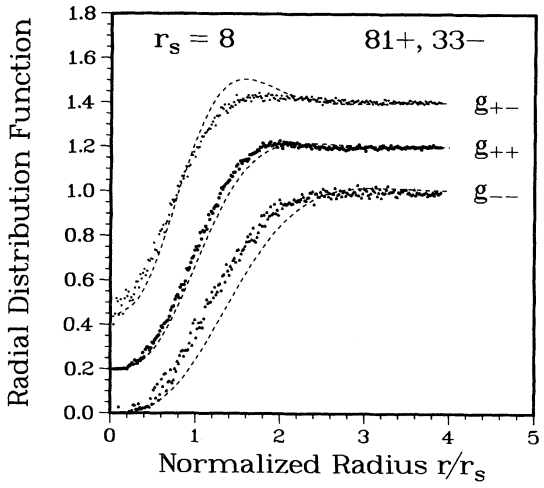

FIG. 1. Example of the radial distribution functions for $r_s = 8$ as collected from $\sim 5 \times 10^5$ attempted steps, before smoothing. The dashed lines are from the Perdew-Wang model, as in the following figures. For clarity, g_{++} and g_{+-} are displaced by 0.2 and 0.4, respectively.

Gaussian factor with full width at half maximum of $\sim 2\Delta x$.

V. RESULTS

We confine our studies here to values of $r_s = \frac{1}{2}$ to 8, corresponding to a density range of $16^3 = 4096$ that spans the range of most interest in solids. In cesium the valence density corresponds to $r_s = 5.6$, in aluminum $r_s = 2$, and in $3d$ transition-metal atoms the spin-polarized d states can sample regions corresponding to $r_s \sim \frac{1}{2}$. We have performed calculations for $r_s = \frac{1}{2}$, 1, 2, 4, and 8, and only representative results are presented here.

A. Partially polarized ($\zeta = 0.42$) case

The calculated RDF's for $\zeta = 0.42$ and 114 electrons (81 up, 33 down) for $r_s = \frac{1}{2}$, 2, and 8 are displayed in Fig. 2 and compared with those resulting from the model of Perdew and Wang. The RDF's in each figure are displaced consecutively by 0.2 units for clarity, and each approaches unity for $x \equiv r/r_s \sim 2$ and beyond. For $r_s = \frac{1}{2}$, where correlation effects are weakest, the agreement is excellent. The calculated antiparallel RDF appears to be slightly lower than the Perdew-Wang (PW) model for $x \sim 1-2$, but the difference is within the statistical uncertainty. Statistical uncertainty precludes any clear conclusion in the interesting region $x \to 0$. Specifically, we conclude that here and for other cases we discuss below the VMC results for $g_{+-}(0)$ and $g'_{+-}(0)$ are not inconsistent with the PW value.

For $r_s = 1$ (not shown) the VMC and PW results are still very close. For decreasing densities $r_s \to 2, 4, 8$ differences between the VMC and PW RDF's become successively larger. For these values of r_s, g_{++} rises noticeably above unity around $x \sim 1.8$. Possibly the minority RDF g_{--} does as well, but more notably it reaches its

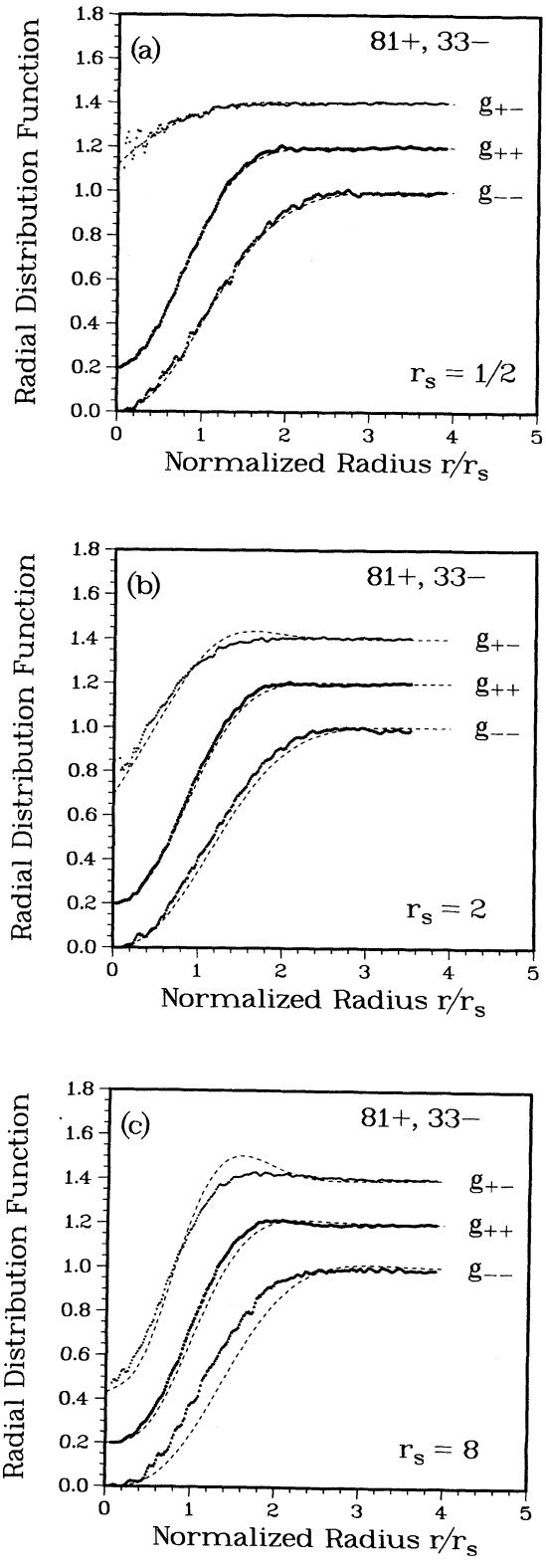

FIG. 2. Smoothed (see text) radial distribution functions for the 81+,33− case, for r/r_s over the interesting region. Relative displacements are as in Fig. 1. Symbols: VMC results; dashed line: Perdew-Wang model. Panels (a)–(c) correspond to $r_s = \frac{1}{2}$, 2, 8. Panel (c) is the smoothed version of Fig. 1.

maximum at larger distance, near $x \sim 2.4$. PW did not attempt to reproduce the $2k_F r$ oscillations in their model, which may account for its lack of an overshoot in the parallel-spin RDF's and exaggerated overshoot in the antiparallel RDF. When a parallel-spin RDF does not overshoot unity, it will satisfy the sum rule equation (13) by compensating (being larger) at smaller x. Although it is not very obvious in Fig. 2 because of the displacement of the curves, the shapes of g_{++} and g_{--} are quite different, and this *difference* is very similar in the VMC results and the PW model.

The antiparallel VMC and PW RDF's show increasing discrepancy as r_s increases. The PW model overshoots unity in the region $x \sim 2$ while the VMC results show little or perhaps no such overshoot. At this time it is not certain whether this difference is an artifact of the PW model or a shortcoming of the VMC correlation factor. The VMC RDF is very smooth until it becomes quite noisy around $x \sim 0.3-0.4$. As mentioned above, no straightforward extrapolation to $x \to 0$ is convincing, but the VMC results are certainly not inconsistent with the PW model values.

The density dependence of the parallel spin RDF's in the PW model is quite small. The increasing difference between the VMC and PW curves as r_s increases reflects almost entirely the change with density of the VMC results: as the density decreases, g_{ss} decreases for $x < 2$ somewhat more than simple scaling with r/r_s would imply. This decrease, and the concomitant overshoot, is perhaps to be expected as the electrons become more correlated at lower density. The PW value of the opposite spin overlap, $g_{+-}(0)$, decreases strongly, from 0.72 at $r_s = \frac{1}{2}$ to 0.03 at $r_s = 8$. Lack of the required statistics at small r restricts our current VMC calculations from making useful predictions on the behavior of $g_{+-}(0)$, except to indicate general consistency with the Perdew-Wang values.

B. Unpolarized case

For the unpolarized case, also with 114 electrons, the corresponding results are shown in Fig. 3. For consistency both g_{++} and g_{--} are shown as calculated. Comparison of the VMC results and PW model follows the same trends as in the partially polarized case, that is, good agreement at high density, with discrepancies increasing as the density decreases and correlation effects grow.

A feature in common with the partially polarized results (and with the fully polarized case, below) is that the VMC RDF is smaller at larger $x \sim 3$, compensating the relatively larger value at $x \sim 1-1.5$. This distinction suggests that the potential energy in the PW model will be smaller than in the VMC calculations. Conversely, the VMC kinetic energy may attain a smaller value than in the PW model arising from the oscillation, i.e, the involvement of fewer short-wavelength components. Due to the complications mentioned in Sec. III, we have not been able to carry out finite-size-scaling studies to check these conjectures.

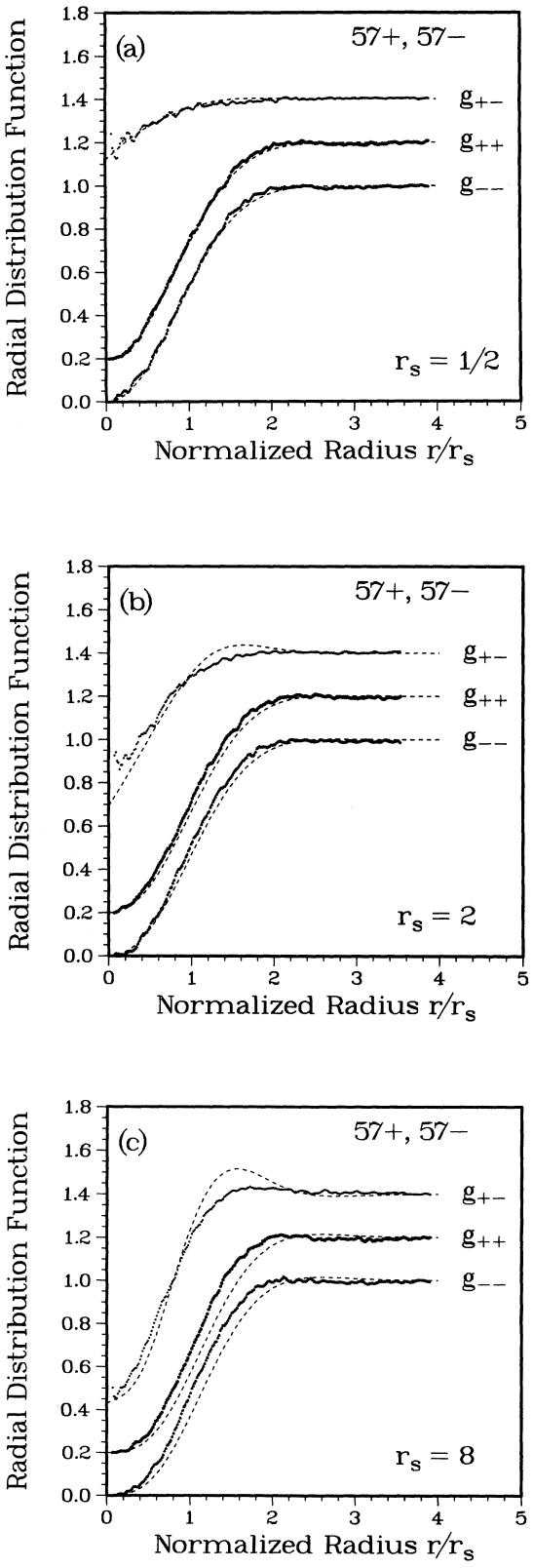

FIG. 3. Radial distribution functions for the unpolarized 57+,57− case analogous to Fig. 2, for $r_s = \frac{1}{2}$, 2, 8. Notation is as in Fig. 2.

In Fig. 4 we show the differences $\Delta g_{ss'} = g_{ss'}(\zeta=0.42) - g_{ss'}(\zeta=0)$ for $r_s=4$. The displacement of Δg_{++} (Δg_{+-}) relative to Δg_{--} is 0.2 (0.8), chosen to separate the curves conveniently. Each approaches zero at $x \sim 4$. In spite of the fact that the VMC and PW parallel-spin RDF's do not agree precisely, this figure shows that they give very similar polarization dependencies. The polarization dependence of the antiparallel-spin RDF is vanishingly small in both cases.

C. Fully polarized case

In Fig. 5 the corresponding results are shown for a fully polarized electron gas with $r_s=4$, simulated with 203 particles. The agreement in RDF's (only a single, parallel-spin RDF in this case) between the VMC calculations and the PW model is very close. Note the (just visible) oscillation and dip in the VMC results below the PW curve near $x \sim 2$, which compensates for the slightly higher value in the $x \sim 1.5$ range. Since what discrepancies there are between VMC and PW have shown up by $r_s=4$ for $\zeta=0$ and $\zeta=0.421$, we expect little if any disagreement for $r_s=8$ for the fully polarized case, so we have not performed that calculation.

D. Total radial distribution function

Since the aim of Perdew and Wang in constructing their model RDF's was to reproduce the total correlation energy, and this function can be written solely in terms of the total RDF, a comparison of the total RDF's to the VMC results may be illuminating. In fact, Perdew and Wang actually modeled only the total RDF, and obtained the partial RDF's from approximate scaling relations for parallel spins, and determining the antiparallel RDF to satisfy Eq. (14). Thus comparing total RDF's is the only completely fair comparison with the Perdew-Wang model. The total RDF's [constructed from Eq. (14) for the VMC results] are shown in Fig. 6 for both the polarized

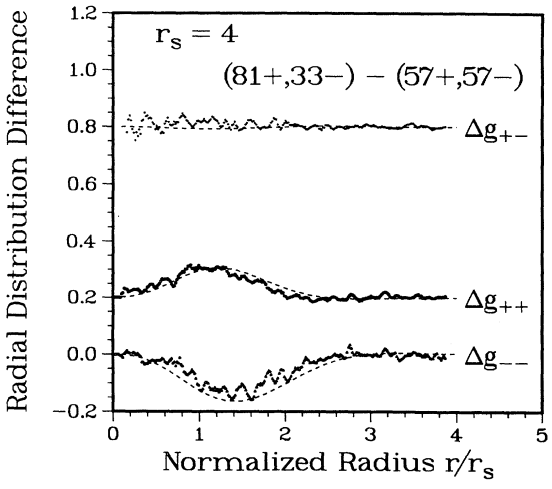

FIG. 4. The difference between polarized and unpolarized radial distribution functions for $r_s=4$. Symbols: VMC calculations; dashed lines: Perdew-Wang model. The $++$ and $+-$ results are displaced by 0.2 and 0.8, respectively, for clarity.

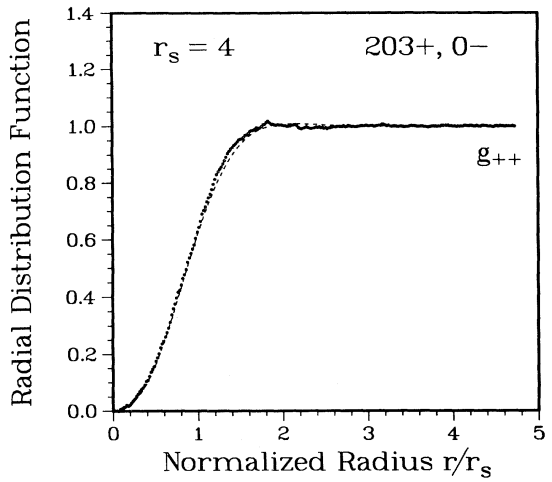

FIG. 5. Radial distribution function for the fully polarized case, with $r_s=4$. Symbols: VMC calculation; dashed line (almost hidden): Perdew-Wang model.

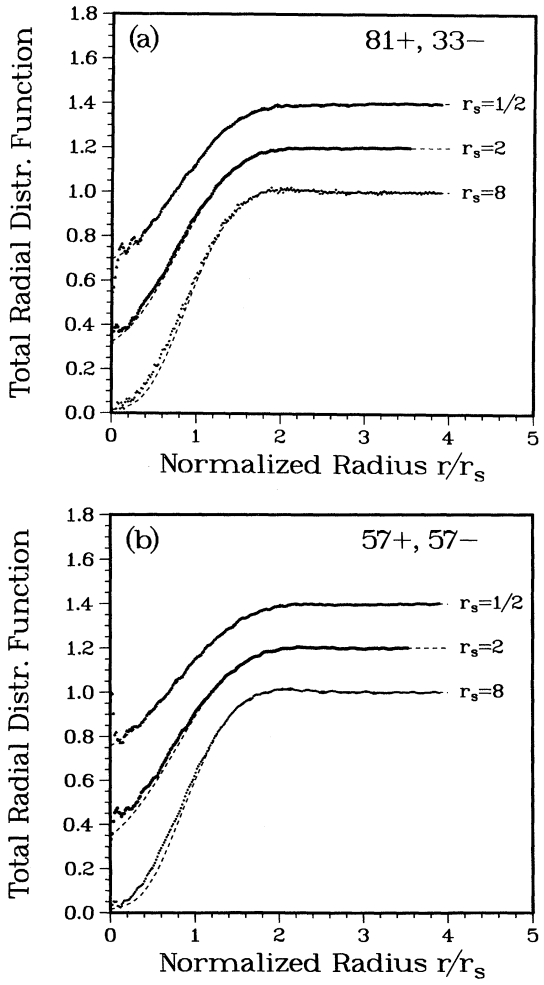

FIG. 6. Total radial distribution function for $r_s=\frac{1}{2}$, 2, and 8, for (a) the polarized case, and (b) unpolarized case. The curves are displaced by 0.2 units for clarity.

and unpolarized cases. For $r_s=\frac{1}{2}$ there is no noticeable difference. For $r_s=2$ the VMC results are slightly larger in the region $x<1$, and the difference becomes more obvious for $r_s=8$. This figure vividly illustrates the strong decrease in $g(0)$ with decreasing density (but recall that the range of density in Fig. 6 is $16^3=4096$).

E. Supercell size dependence

A possible dependence of the VMC results on the number of particles in the simulation should be addressed; after all, 114 particles correspond only to a roughly $5\times5\times5$ arrangement on average. To investigate possible size dependence we have calculated the RDF's for $r_s=4$ using 284 particles (203+,81−). This choice was made because the polarization is $\zeta=122/284=0.430$, very close to the 81+,33− case we had already calculated which has $\zeta=0.421$. The RDF's are indistinguishable from the 81+,33− case and are not shown. We conclude that the current VMC results for the RDF's are limited somewhat by statistics but not by simulation cell size.

VI. DISCUSSION

There are relatively few previous results with which to compare our RDF's. It is instructive to consider the lowest-order approximation, the Hartree-Fock (HF) approximation. In HF opposite spin electrons are uncorrelated: $g_{+-}(r)=1$. The parallel-spin RDF's are given by

$$g_{ss}(r)=1-\left[3\frac{\sin y-y\cos y}{y^3}\right]^2\Bigg|_{y=k_{F,s}r} \tag{19}$$

and since $k_{F,s}\sim1/r_s$, this function is a universal function of $x=r/r_s$. [For the unpolarized case $r_sk_F=(9\pi/4)^{1/3}=1.919$.] The HF results become exact in the high density ($r_s\to0$) limit. Figures 2 and 3 confirm that the density dependence of the parallel-spin RDF's is not strikingly different from an r/r_s scaling up to $r_s=8$; of course the antiparallel RDF differs strongly at small r from the HF of unity except at very high density.

The HF RDF's are contrasted with those of the PW model and VMC calculations in Fig. 7 for $r_s=8$. One difference is the k_Fr oscillations, which are just visible in the HF parallel-spin RDF's and are expected to be reduced by correlation. Perdew and Wang did not attempt to model these oscillations, since they are not anticipated to be crucial in determining the correlation energy. Our VMC calculations cannot accurately reproduce k_Fr oscillations either, because they arise from the sharpness of the Fermi surface and the Fermi sphere is sampled only discretely in our supercell calculation. Another feature of the HF RDF for parallel spins is that it never exceeds unity, but there is no formal restriction against $g_{ss}(r)$ exceeding unity.

Figure 7 indicates to what extent the correlation modeled in the Perdew-Wang RDF results in a larger exchange-correlation hole than is obtained in the present VMC calculations. Over much of the range $0<x<2$ the difference is roughly twice as large for PW as for VMC. It is worthy of note that the small amplitude oscillation of $g_{++}(r)$ in the $2<x<3$ range in the Hartree-Fock RDF seems to be reproduced by the VMC calculation. A more careful statistical analysis would be necessary to establish this beyond doubt.

An important question (and one not seriously addressed in this study) is: what are the limitations of the VMC method? The approximate nature of the wave function has two distinct (but perhaps related) consequences. First, the expectation value of the energy is not guaranteed to be accurate, but only an upper bound, and second, the variance of the (local) energy is nonzero. Although the energies have not been our concern here, we gain some insight into the difficulties by monitoring the kinetic energy, in the three forms F^2, T, and $K=2T-F^2$ discussed in Sec. II. In a sequence of 2000 Monte Carlo steps (a very short run) in a fully equilibrated system the

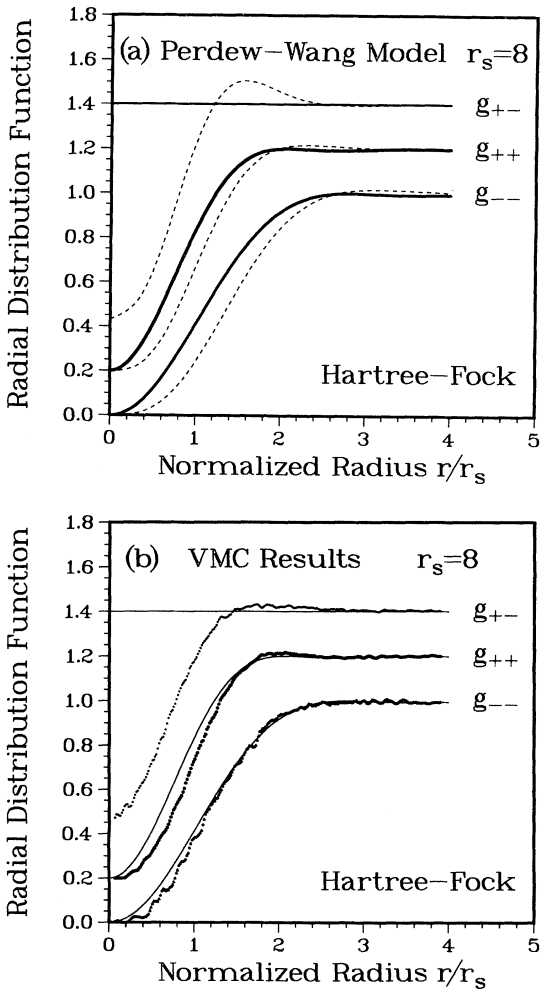

FIG. 7. Comparison of the Hartree-Fock radial distribution function (heavy lines) with (a) the Perdew-Wang model and (b) variational Monte Carlo results for $r_s=8$, which are the same as in Fig. 1(d). Curves are displaced for 0.2 units for clarity. The Perdew-Wang RDF's differ from Hartree-Fock somewhat more than do the VMC results. Note that the k_Fr oscillations in the Hartree-Fock curves are just visible.

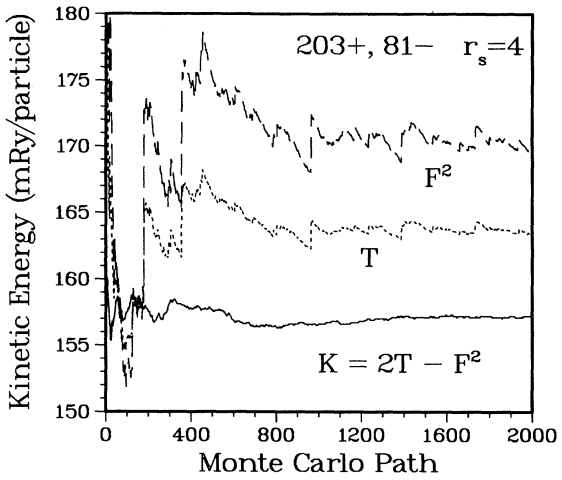

FIG. 8. Cumulative averages of the three expressions for the kinetic energy, T, F^2, and $K=2T-F^2$, for a short simulation. Certain steps result in large changes in energy, suggesting that particular regions of the wave function contribute inordinately to the variance of the energy. Note that K is a far superior expression for evaluating the kinetic energy.

running average value of each of these quantities is plotted in Fig. 8. The means of all three of these quantities must finally be equal (independent of the quality of the wave function), and indeed we find them to be equal within their variances (this is not evident from Fig. 8). Figure 8 illustrates why the variance of K is so much smaller than that of T (typically 3–5 times larger) and F^2 ($\sim$10 times larger): the large variations in energy usually have the same sign in T and F^2 and therefore strongly cancel in K. The more illuminating feature of Fig. 8 is that it suggests that the variance of the kinetic energy may be dominated by certain regions where the wave function is particularly poor. At this point we have not determined which configurations are sampling these difficult regions, i.e., how to characterize these regions.

VII. SUMMARY

We have applied the variational Monte Carlo method to study the polarization dependence of the spin-resolved radial distribution functions in the electron gas. Our results extend the knowledge of the RDF's beyond the results for the unpolarized[17] and fully polarized[18] electron gases, both based on coupled clusterlike methods. For parallel spins the exchange-correlation hole is somewhat larger than the Hartree-Fock result but less extended than the model of Perdew and Wang. For the antiparallel RDF the VMC result is less structured than that of Perdew and Wang. In both cases the differences are small at high density ($r_s=0.5-1$) but become pronounced for $r_s=4-8$. The present results support earlier suggestions (for example, Rajagopal, Kimball, and Manerjee[16]) that the correlation energy is more sensitive to the antiparallel-spin RDF g_{+-} than to the parallel-spin RDF, so that particular attention should be given to improving the antiparallel correlation factor in the Jastrow-Slater wave function.

With the continuing discoveries of important materials that are not well described by the local density approximation or even the generalized gradient approximation (GGA) to density-functional theory, there is increasing reason to proceed to a fully nonlocal exchange-correlation functional. Fahy, Wang, and Louie[10] have performed pioneering work on the position dependence of the RDF in diamond and silicon, but most of the serious deficiencies of the LDA and GGA occur in magnetic, or nearly magnetic, materials rather than the simpler, nonmagnetic materials. A prime candidate to give qualitative improvement is the weighted density approximation, whose implementation requires a knowledge of the (coupling-constant-averaged) pair correlations that are the topic of this paper. The study of pair correlations in the polarized electron gas must be continued to supply the necessary input to such calculations. In this way we may learn how far one can proceed in the description of real, inhomogeneous materials using a theory based on the homogeneous electron gas.

ACKNOWLEDGMENTS

We thank J. P. Perdew for providing a program to calculate the model radial distribution function of Ref. 7, and for several communications on this topic. J. P. Perdew and P. J. Reynolds provided helpful comments on the manuscript. We acknowledge useful conversations with J. W. Serene and D. W. Hess in the early stages of this work. This research was supported by Office of Naval Research Contract No. N00014-93-WX-24012. Some of the computations were carried out at the Cornell National Supercomputing Facility.

[1]D. Ceperley, Phys. Rev. B **18**, 3126 (1978).
[2]C. J. Umrigar, K. G. Wilson, and J. W. Wilkins, Phys. Rev. Lett. **60**, 1719 (1988).
[3]S. Fahy, X. W. Wang, and S. G. Louie, Phys. Rev. Lett. **61**, 1631 (1988); Phys. Rev. B **42**, 3503 (1990).
[4]D. Ceperley and B. J. Alder, Phys. Rev. Lett. **45**, 566 (1980).
[5]P. J. Reynolds, D. M. Ceperley, B. J. Alder, and W. A. Lester, Jr., J. Chem. Phys. **77**, 5593 (1982).
[6]J. G. Zabolitzky, Phys. Rev. B **22**, 2353 (1980).
[7]J. P. Perdew and Yue Wang, Phys. Rev. B **46**, 12 947 (1992). Note that these authors constructed their model for the coupling-constant-averaged radial distribution function. The physical value used in this paper is obtained from the differential relationship given in their Eq. (7).
[8]G. Ortiz and P. Ballone, Europhys. Lett. (to be published).
[9]J. P. Valleau and S. G. Whittington, in *Statistical Mechanics*, edited by B. J. Berne (Plenum, New York, 1977), Pt. A, p. 137.
[10]N. Metropolis, A. W. Rosenbluth, M. N. Rosenbluth, A. H. Teller, and E. Teller, J. Chem. Phys. **32**, 1087 (1953).
[11]S. G. Louie, in *Atomic Scale Calculations in Materials Science*, edited by J. Tersoff, D. Vanderbilt, and V. Vitek, MRS Symposia Proceedings No. 141 (Materials Research Society, Pittsburgh, 1989), p. 3.

[12]S. Fahy, X. W. Wang, and S. G. Louie, Phys. Rev. Lett. **65**, 1478 (1990).
[13]X. W. Wang, J. Zhu, and S. G. Louie, Phys. Rev. Lett. **65**, 2414 (1990).
[14]T. Kato, Commun. Pure Appl. Math. **10**, 151 (1957).
[15]J. C. Kimball, Phys. Rev. A **7**, 1648 (1973); J. Phys. A **8**, 1513 (1973).
[16]A. K. Rajagopal, J. C. Kimball, and M. Manerjee, Phys. Rev. B **18**, 2339 (1978).
[17]F. A. Stevens, Jr. and M. A. Pokrant, Phys. Rev. B **8**, 990 (1973).
[18]J. G. Zabolitzky, Phys. Rev. B **22**, 2353 (1980).